2022 30th Mediterranean Conference on Control and Automation (MED)
June 28 - July 1, 2022. Athens, Greece

2022 30th Mediterranean Conference on Control and Automation (MED) | 978-1-6654-0673-4/22/$31.00 ©2022 IEEE | DOI: 10.1109/MED54222.2022.9837131

PWA-CTM: An Extended Cell-Transmission Model based on Piecewise Affine Approximation of the Fundamental Diagram

Fatemeh Alimardani and John S. Baras

Abstract— **Throughout the past decades, many different versions of the widely used first-order Cell-Transmission Model (CTM) have been proposed for optimal traffic control. Highway traffic management techniques such as Ramp Metering (RM) are typically designed based on an optimization problem with nonlinear constraints originating in the flow-density relation of the Fundamental Diagram (FD). Most of the extended CTM versions are based on the trapezoidal approximation of the flow-density relation of the Fundamental Diagram (FD) in an attempt to simplify the optimization problem. However, this relation is naturally nonlinear, and crude approximations can greatly impact the efficiency of the optimization solution. In this study, we propose a class of extended CTMs that are based on piecewise affine approximations of the flow-density relation such that (a) the integrated squared error with respect to the true relation is greatly reduced in comparison to the trapezoidal approximation, and (b) the optimization problem remains tractable for real-time application of ramp metering optimal controllers. A two-step identification method is used to approximate the FD with piecewise affine functions resulting in what we refer to as PWA-CTMs. The proposed models are evaluated by the performance of the optimal ramp metering controllers, e.g. using the widely used PI-ALINEA approach, in complex highway traffic networks. Simulation results show that the optimization problems based on the PWA-CTMs require less computation time compared to other CTM extensions while achieving higher accuracy of the flow and density evolution. Hence, the proposed PWA-CTMs constitute one of the best approximation approaches for first-order traffic flow models that can be used in more general and challenging modeling and control applications.**

I. Introduction

Optimal traffic control has been extensively studied since the beginning of the twentieth century, and is still a topic of ongoing research. Towards this direction, numerous traffic flow models have been developed and used to understand, describe, and predict traffic flow in different real-life scenarios, ranging from bi-directional roads to multi-lane highways with on-ramps [1], [2], [3].

Traffic flow models constitute dynamical models that can be classified as micro-, meso- or macroscopic models, depending on whether the model distinguishes the behavior of each individual vehicle or makes use of mean-field limit metrics [4]. In particular, the main advantage of macroscopic traffic models over microscopic models is the significantly lower computational costs due to lower complexity [5]. These models are typically described by the traffic density (average number of vehicles per unit length of road) and flow (average number of vehicles per time unit) and can be further categorized with respect to the underlying model dynamics into first order or second order models. The most frequently used macroscopic traffic flow models are first order models, such as the Lighthill-Whitham-Richards (LWR) model [6], which is a continuous model, and the Cell-Transmission Model (CTM) [7] which is a discretized version of the LWR model. The simplicity and computational benefits of the CTM has given rise to many CTM extensions, each one proposed based on different criteria and the specific needs of different applications. A review of the different CTM extensions and versions proposed over the years can be found in [8]. In [9], two of the mostly used CTM versions, namely the linear relaxation of CTM [10] and the extended CTM [8] are thoroughly evaluated. Throughout the manuscript, we will refer to these models as the *Relaxed* and the *Extended* CTM versions, respectively.

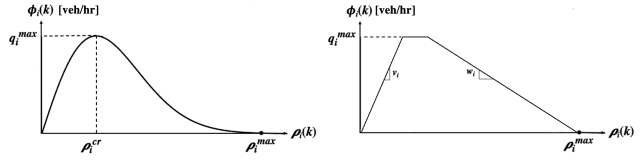

Fig. 1: The original (non-linear) Fundamental Diagram (FD) [11] *(left)* and its trapezoidal approximation [12] *(right)*.

Many highway traffic management techniques, such as autonomous traffic signal control (Ramp Metering) [1], [2], are formulated as optimization problems with constraints originating in this flow-density relation of the fundamental diagram. However, in order to reduce the complexity of such methods, most of the CTM versions are based on triangular [13] or trapezoidal approximation [12] of the flow-density relation of the fundamental diagram. The trapezoidal FD is more commonly used in the literature and is shown in Fig. 1. Due to the fact that the flow-density relation is naturally a nonlinear relation (Fig. 1), crude approximations of the fundamental diagram can greatly impact the efficiency of the optimization solution, and, as a result, the performance of the traffic control methodology. On the other hand, control algorithms that take into account the original non-linear FD, are computationally expensive and typically not suited for real-time application. In [9], it was shown that optimization problems based on the *Relaxed CTM* did indeed have computational advantages, while finite horizon optimal control problems (FHOCPs) based on the more complicated *Extended CTM* model showed better traffic

The authors are with the Electrical and Computer Engineering Department and the Institute for Systems Research, University of Maryland, College Park, USA. emails:{fatimalm, baras}@umd.edu

Research partially supported by ONR grant N00014-17-1-2622.

control performance but reduced computational efficiency. In other words, there exists a trade-off between performance and complexity for the CTM-based traffic control algorithms, which has its roots on the approximation accuracy of the fundamental diagram.

In this work, we propose a class of extended CTMs that are based on piecewise affine approximations of the flow-density relation of the fundamental diagram (FD) such that:

(i) the integrated squared error with respect to the true relation is greatly reduced in comparison to the trapezoidal approximation, and
(ii) the optimization problem remains tractable for real-time application of ramp metering optimal controllers.

A two-step identification method is used to approximate the FD with piecewise affine functions resulting in new extensions of the CTM that we will refer to as *PWA-CTM* traffic flow models. The proposed models are evaluated in the framework of finite horizon optimal control problems using ramp metering controllers, e.g. the widely used PI-ALINEA approach, in complex highway traffic networks. Hence, the proposed PWA-CTM models constitute one of the best approximation approaches for first-order traffic flow models that can be used in any finite horizon optimal control problem to enhance its performance regarding the computational time and the convergence to the equilibrium state.

The paper is organized as follows: The CTM traffic flow model, different flow-density relations of the FD, and the ramp metering control scheme used in this study are briefly defined in Section II. In Section III, a two-step piecewise affine identification of nonlinear systems is described and applied to the nonlinear flow-density relation of the FD to find its PWA approximation. Also, the new CTM extensions based on this approximation of the FD are proposed in this section. The formulation of the FHOCPs are explained in Section IV and in Section V the simulation results are reported and analysed in detail. Finally, some conclusive remarks are drawn in Section VI.

II. Preliminaries

In this section, we briefly introduce the Cell-Transmission Model (CTM), illustrate the importance of the fundamental relation between flow and density that constitutes the Fundamental Diagram (FD), and define a broadly used Ramp Metering (RM) control method to be used in our experiments.

A. The CTM model

The Cell Transmission Model (CTM) is a popular numerical method originally proposed by Carlos Daganzo [7], [13] to solve the kinematic wave equation. CTM models can be used to predict the macroscopic traffic behavior on a given road lane, by evaluating the traffic flow ϕ_i and density ρ_i at a finite number of intermediate points that result from dividing the lane into homogeneous sections $i \in [1, 2, \ldots, N]$ (hereafter called cells), as shown in Fig. 2. All notations used in this work, including all the model

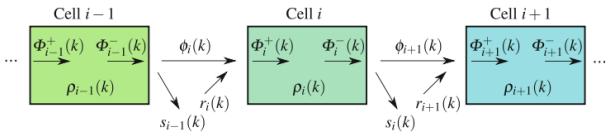

Fig. 2: Sketch of a freeway stretch in the CTM [8].

variables and parameters, are explained in table I and the schematic of Fig. 2. Detailed explanation about the notation can be found in [8] and [9].

Initial and boundary conditions are appropriately defined to iteratively evaluate the values of the quantities at each cell. The flow across the cells is determined based on ϕ_i and ρ_i, which are the two monotonic functions that uniquely define the fundamental diagram (FD) as shown in Fig. 1. The update equations are given by:

$$\rho_i(k+1) = \rho_i(k) + \frac{T}{L}(\Phi_i^{+}(k) - \Phi_i^{-}(k)) \tag{1}$$

$$\Phi_i^{+}(k) = \phi_i(k) + r_i(k) \tag{2}$$

$$\Phi_i^{-}(k) = \phi_{i+1}(k) + s_i(k) \tag{3}$$

$$s_i(k) = \frac{\beta_i(k)}{1-\beta_i(k)}\phi_{i+1}(k) \tag{4}$$

$$l_i(k+1) = l_i(k) + T(d_i(k) - r_i(k)) \tag{5}$$

For uncontrolled on-ramps:

$$r_i(k) = d_i(k), \quad 0 \le r_i(k) \tag{6}$$

and, for controlled on-ramps:

$$r_i(k) \le l_i(k) + d_i(k), \quad 0 \le r_i(k) \le r_i^{C,max} \tag{7}$$

The boundary conditions are given by:

$$0 \le \rho_i(k) \le \rho_i^{max}(k) \tag{8}$$

$$0 \le \phi_i(k) \le q_i^{max}(k) \tag{9}$$

$$0 \le l_i(k) \le l_i^{max} \tag{10}$$

The flow variable $\phi_i = f(\rho_i)$ is given by the fundamental diagram (FD) which will be described in the next section. For a detailed overview of the model, the readers are referred to [8].

B. Fundamental Diagram and the Trapezoidal Approximation

A key feature of the CTM is the assumption that there is some fundamental relation between the density and the flow variables, i.e.,

$$\phi_i = f(\rho_i) \tag{11}$$

This relation is known as the Fundamental Diagram (FD). Three families of this functional form have been proposed throughout the past decades: 1) Linear forms first proposed by Greenshields [14], 2) Nonlinear forms using logarithmic [15] or exponential form [11], [16], and 3) Multi-regime forms which use rather simple functional forms, e.g. linear or

TABLE I: Model Variables and Parameters

Symbol	Description/Unit (Range)
N	Number of cells / int
i	Cell index / $i = \{1, ..., N\}$
T	Sampling period / (h)
K	Time Horizon / int
k	Time index / $k = \{0, ..., K-1\}$
L_i	Length of each cell / (km)
v_i^f	Free-flow speed of cell i / (km/h)
w_i	Congestion wave speed / (km/h)
a_i	A parameter to be estimated from empirical data
q_i^{max}	Cell capacity / (veh/h)
λ_i	Lane numbers / int
$\rho_i(k)$	Traffic density / (veh/km)
ρ_i^{cr}	Critical density / (veh/km)
ρ_i^{max}	Jam density / (veh/km)
$\phi_i(k)$	Mainstream flow / (veh/h)
$\Phi_i^+(k)$	Total flow entering cell i / (veh/h)
$\Phi_i^-(k)$	Total flow exiting cell i/ (veh/h)
$l_i(k)$	Queue length in the on-ramp /(veh)
l_i^{max}	Maximum on-ramp queue length / (veh)
$r_i(k)$	Flow entering mainline from the on-ramp / (veh/h)
$r_i^C(k)$	Ramp metering control variable / (veh/h)
$r_i^{C,max}$	Maximum metering rate / (veh/h)
r_i^*	Ramp metering set point / (veh/h)
$d_i(k)$	Demand flow accessing the on-ramp / (veh/h)
$s_i(k)$	Flow exiting mainline through the off-ramp / (veh/h)
$\beta_i(k)$	Split ratio / $\in [0, 1]$
K_R	Integral regulator gain
K_P	Proportional regulator gain

quadratic functions, for intervals of density [17], [18]. The interested reader can find a precise review of FDs in [12] and [19]. Equation (12) reads the exponential flow-density relation (Fig. 1).

$$\phi_i(k) = \rho_i(k) * v_i^f \exp[-\frac{1}{a_i}(\frac{\rho_i(k)}{\rho_i^{cr}})^{a_i}]; \tag{12}$$

In some models, a different steady-state relation is considered for each cell i. The trapezoidal FD (Fig. 1) belongs to the third family of FD models and is described by eq. (13).

$$\begin{aligned}\phi_i(k) = \min\{&v_{i-1}^f(\rho_{i-1}(k) + r_{i-1}(k)), q_{i-1}^{max}, \\ &w_i(\rho_i^{max} - \rho_i(k) - r_i(k))\}\end{aligned} \tag{13}$$

In this study, the goal is to find a linear approximation of the FD which would have closer behavior to the nonlinear relation (12) but would make the constraints of optimization-based problems linear as the trapezoidal approximation (13) does.

C. Ramp Metering Control

Ramp metering (RM) is achieved by placing traffic signals at on-ramps to control the flow rate at which vehicles enter the freeway. The ramp metering controller computes the metering rate to be applied. PI-ALINEA is a feedback local ramp metering strategy proposed by [20] and it is indeed a proportional-integral feedback control algorithm, in which the metering rate is given by

$$r_i^C(k) = r_i^C(k-1) + K_R[\rho_i^* - \rho_i(k)] - K_P[\rho_i(k) - \rho_i(k-1)] \tag{14}$$

where the flow that can enter section i of a freeway from the on-ramp of cell i during time interval $[kT, (k+1)T)$ is represented by $r_i^C(k)$. In case the main objective of the traffic controller is to reduce congestion and to maximize the throughput (see Section IV), a good choice for the set-point is $\rho_i^* = \rho_i^{cr}$.

III. Two-Step Piece-wise Affine Identification of Nonlinear Systems

In this section we consider a nonlinear function $f : \Omega \to \mathbb{R}$, $\Omega \subseteq \mathbb{R}$, and describe a two-step optimization-based approach to find a piece-wise affine (PWA) function:

$$\tilde{f} = \sum_{i=1}^{M} \mathbb{1}_{[x \in R_i]}(a_i x + c_i) \tag{15}$$

such that the approximation error $e = \|f - \tilde{f}\|^2$ is minimized. Here, the regions $\{R_i\}_{i=1}^M$ define a partition of Ω, $\mathbb{1}_{[\cdot]}$ represents the indicator function, and $\|f\|^2 = \int_\Omega |f(x)|^2 dx$ denotes the L^2 norm. The optimal parameters $\{a_i\}_{i=1}^M$, $\{c_i\}_{i=1}^M$, and $\{R_i\}_{i=1}^M$, are the output of the optimization process that minimize the approximation error e.

Following the two-step identification process described in [21], we split the search for the PWA function $\tilde{f}$ into two steps. In the first stage we will approximate the function f with an analytic function $\hat{f} : \Omega \to \mathbb{R}$ of known form and lower complexity, by minimizing the error $\hat{e} = \|f - \hat{f}\|^2$. In the second step, an optimization-based procedure will be applied to derive an optimal PWA approximation $\tilde{f}$ such that the approximation error $\tilde{e} = \|\hat{f} - \tilde{f}\|^2$ is minimized. Assuming that $\Omega = [\underline{k}, \bar{k}]$, the partition $\{R_i\}_{i=1}^M$ of M non-overlapping parts is described by the regions $R_1 = [\underline{k}, r_1]$, $R_2 = [r_1, r_2]$, ..., $R_M = [r_{M-1}, \bar{k}]$, with $\bigcup_i R_i = [\underline{k}, \bar{k}]$. Then, the problem reduces to finding the slopes $a_i \in \mathbb{R}$, offsets $c_i \in \mathbb{R}$ and breakpoints $r_i \in \mathbb{R}$ such that the approximation error $\tilde{e}$ is minimized, i.e.

$$\min_{\{a_i, c_i, r_i\}} \sum_{i=1}^{M} \left(\int_{r_i - 1}^{r_i} (f(x) - (a_i x + c_i))^2 dx \right) \tag{16}$$

s.t.

$$\underline{k} \leq r_1 \leq \ldots \leq r_{M-1} \leq \bar{k} \tag{17}$$

$$a_i r_i + c_i = a_{i+1} r_{i+1} + c_{i+1}, \quad i = 1, \ldots, M-1 \tag{18}$$

To implement the first step, the exponential flow-density function $\phi_i = f(\rho_i)$ is approximated by a polynomial function of different degrees $n \in \{3, \ldots, 6\}$. Considering the trade-off between the complexity of the resulting polynomials and the mean squared error (MSE) of the approximation, the optimal polynomial degree was chosen as $n = 5$ for this step. For reproducibility and future reference, we provide the coefficients of the polynomial approximation in eq. (19) below:

$$\phi_i(k) = \hat{f}_{p_5}(\rho_i(k)) = \textstyle\sum_{j=0}^{5} c_j \rho_i(k)^j \tag{19}$$

where $\{c_j\}_{j=0}^5 = \{373.77, 1249.24, 1110.26, 95.83, 436.69, 118.43\}$. The approximation function $\hat{f}$ is compared against the flow-density relation f in Fig. 3, as well, where we have set $\Omega = [0, 180]$.

For the second step, the optimization problem in (16), (17), (18) was solved, and the optimal, in terms of MSE,

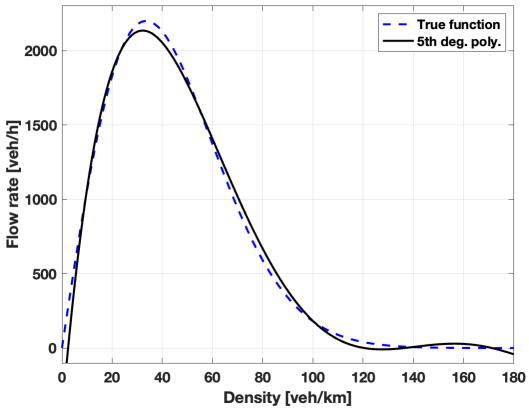

Fig. 3: 5th-degree polynomial approximation of the FD.

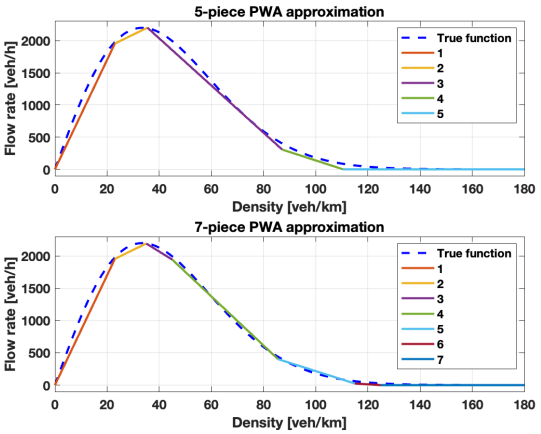

Fig. 4: 5- and 7-Piece PWA approximation of the FD.

number of pieces $M \in \{5, 6, 7\}$ was chosen. The MSE of the approximations of the flow-density function are provided in table II. Interestingly, in this problem, increasing the number of pieces does not necessarily translate to a similar decrease in the MSE (see table II). The approximation with $M = 6$ pieces showed higher MSE. As a result, for this phase, the approximations with $M = 5$ and $M = 7$ pieces will be considered in the experimental section that follows to develop new CTMs. Figure 4 shows the comparison between these PWA functions and the true fundamental diagram. Also, for reproducibility, the coefficients $\{a_i\}_{i=1}^{M}$, $\{c_i\}_{i=1}^{M}$, and $\{r_i\}_{i=1}^{M-1}$ of the functions $\phi_i = \tilde{f}_5(\rho_i)$, and $\phi_i = \tilde{f}_7(\rho_i)$ are provided in equations (20) and (21), respectively.

Remark 1: We note that PWA functions with $M > 7$ number of pieces were also investigated but are omitted since the marginal benefit in the performance (resulting MSE) is insignificant compared to the increase in the complexity of the method (and, therefore, the computation time).

TABLE II: MSE of different PWA approximations.

Piece Number	MSE
M=5	6433.14
M=6	7007.30
M=7	4375.17

$$\tilde{f}_5(\rho_i) = \begin{cases} 85.00 * \rho_i, & 0 \le \rho_i \le 23.00 \\ 19.78 * \rho_i + 1499.98, & 23.00 \le \rho_i \le 35.45 \\ -36.66 * \rho_i + 3501.06, & 35.45 \le \rho_i \le 87.12 \\ -13.12 * \rho_i + 1450.00, & 87.12 \le \rho_i \le 110.50 \\ 0, & \text{otherwise} \end{cases} \tag{20}$$

$$\tilde{f}_7(\rho_i) = \begin{cases} 84.99 * \rho_i, & 0 \le \rho_i \le 23.00 \\ 19.99 * \rho_i + 1490.00, & 23.00 \le \rho_i \le 35.00 \\ -20.00 * \rho_i + 2890.00, & 35.00 \le \rho_i \le 45.00 \\ -37.99 * \rho_i + 3700.00, & 45.00 \le \rho_i \le 93.57 \\ -13.90 * \rho_i + 1450.00, & 93.57 \le \rho_i \le 100.00 \\ -2.40 * \rho_i + 300.00, & 100.00 \le \rho_i \le 124.00 \\ 0, & \text{otherwise} \end{cases} \tag{21}$$

Remark 2: In the first step, the exponential flow-density function $\phi_i(k)$ can be approximated by any smooth regression function, e.g. a polynomial function or a feed-forward neural network. It is important to note that this step can be implemented as a data-based optimization algorithm, where actual traffic flow data are used to estimate the optimal fundamental diagram for the road and application at hand. This leads to learning-based traffic control approaches, which lie beyond the scope of this paper.

A. The Piecewise Affine Cell-Transmission Models (PWA-CTMs)

Depending on the PWA approximation of the FD used, the CTM described in Section II-A can be extended to the models *PWA5-CTM* and *PWA7-CTM*, each using a PWA approximation with $M = 5$ and $M = 7$ pieces, respectively. The fundamental flow-rate relation $\phi_i = f(\rho_i)$, is now approximated by eq. (20) for the PWA5-CTM, and by eq. (21) for the PWA7-CTM model.

IV. Finite Horizon Optimal Control Formulation

In this section, four Finite Horizon Optimal Control Problems (FHOCPs) with different underlying traffic flow models are formulated to investigate the evolution of traffic flow in each case. The traffic flow models used here define four different versions of the CTM. Two of the versions used are the Extended CTM [8] and the Relaxed CTM [10]. A thorough assessment on these two models is presented in [9]. The other two CTM versions are the PWA-CTMs proposed in the previous section. The traffic control strategy applied here is the PI-ALINEA ramp metering controller, and the analysis is performed by simulation for a hypothetical network of freeways with stationary demand patterns using the unique equilibrium state of each pattern.

Before developing the formulations of the FHOCPs, first the definitions of two objective functions will be provided. In the formulation of FHOCPs presented in this section, a linear combination of these cost functions will make the final objective of each problem. The most widely used objective in traffic management is to minimize the total time that all

vehicles spend in the network (i.e., the Total Time Spent or TTS). Basically, the TTS is the time spent by all vehicles in the network (i.e., the total travel time or TTT), including the waiting time experienced at origins (i.e., the total waiting time or TWT).

$$J_1 = J_{TTS} = T \sum_{k=0}^{K-1} [\sum_{i=1}^{N} \rho_i(k) L_i \lambda_i + \sum_{i=1}^{N} l_i(k)] \quad (22)$$

The second objective function applied here is to maximize the sum of the traffic flows going through all sections and on-ramps. This objective function is also called the Total Travel Distance (TTD) since it is the total distance (veh mi) covered by all the vehicles in the considered time horizon.

$$J_2 = J_{TTD} = T \sum_{k=0}^{K-1} [\sum_{i=1}^{N} \phi_i(k) L_i + \sum_{i=1}^{N} r_i(k) L_i] \quad (23)$$

A linear combination of these two objective functions is used as the objective function to express their priorities, i.e.

$$\min_{r_i^C} \alpha_1 J_1 - \alpha_2 J_2 \quad (24)$$

Here, $\alpha_1 > \alpha_2$ as minimizing the travel time is the main objective. Also, the α_i values are the same for all four problems.

The different FHOCP problems are defined by optimization problem (24), the controller (14), the constraints (1)-(10), and different flow-density relationship $\{\phi_i = f_j(\rho_i)\}_{j=1}^{4}$ given by:

FHOCP 1: $\phi_i = f_1(\rho_i) \sim$ Extended CTM [8], [9];
FHOCP 2: $\phi_i = f_2(\rho_i) \sim$ Relaxed CTM [9], [10];
FHOCP 3: $\phi_i = f_3(\rho_i) \sim$ (20); and
FHOCP 4: $\phi_i = f_4(\rho_i) \sim$ (21).

V. Simulation Results

In this section, we evaluate the performance and complexity of the proposed methodology on a complex simulation environment.

A. Case study and model parameters

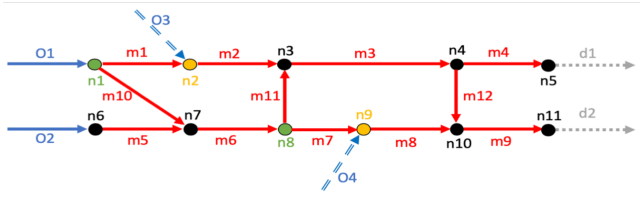

Fig. 5: Complex highway network under consideration.

Simulation is performed for the network shown in Fig. 5 with two origins ($o1$ and $o2$), two controlled on-ramps ($o3$ and $o4$), 12 mainline links ($m1$ through $m12$) and two destinations ($d1$ and $d2$). One assumption about the network is that the proportion of turns at every junction, i.e. the split ratios $\beta_i(k)$, are fixed and known in advance. Also, it is assumed that the behavior of all the links can be described by parameters shown in table III adopted from [9], [22] and converted to SI units for this study:

TABLE III: Model Parameters.

Symbol	Value	Unit/Range
Period T	0.5	min
Length L_i	1	km
v_i	1	length/period
w_i	0.33	length/period
$\bar{n}_i$	180	veh/length
n_i^c	40	veh/length
$\bar{f}_i$	20	veh/period

B. Simulation and Numerical Results

The results of the simulation of the four FHOCPs proposed in section IV are provided in this section. The FHOCPs were solved with Yalmip, the modeling and optimization language offered by [23], and the GURUBI non-commercial optimization solver via the interface of MATLAB. The simulation horizon of 1 hour is considered by choosing the time horizon of K = 120 time steps and the simulation period of T = 0.5 minute ($K * T$ = 60 minute). For the simulation phase of this study, the following stationary demand vector was applied for origin links $o1$ and $o2$ and also on-ramp links $o3$ and $o4$: $d(k) = (8, 9, 7, 3)$ *veh*/0.5 *min*. According to [22], for each stationary demand vector $d(k) = (d_0, ..., d_M)$, there exists a unique equilibrium flow rate $\phi(k) = (q_0, ..., q_N)$ and density vector $\rho(k) = (\rho_0, ..., \rho_N)$. Detailed explanation on the calculation of these vectors is explained in [22]. Table IV shows the theoretical equilibrium flow vector for the mainline links of this network based on the chosen stationary demand. Adding all these values together, the network flow rate at the equilibrium state should be equal to 113.37 *veh*/0.5 *min*. Knowing this theoretical flow vector and having the overall value of the network flow rate provide an insight on what is expected to see in the simulation phase.

TABLE IV: Theoretical equilibrium flow rate (veh/0.5 min) vector.

Link Number	**1**	**2**	**3**	**4**	**5**	**6**
Flow rate	4.8	11.8	15.46	9.27	9	12.2
Link Number	**7**	**8**	**9**	**10**	**11**	**12**
Flow rate	8.54	11.54	17.72	3.2	3.66	6.18

Figure 6 shows the comparison of the network flow rate, i.e. the summation of the flow rate of all the links, in all four FHOCPs during the 1-hour simulation horizon. In all problems, the network flow rate is showing convergence to the value of the theoretical equilibrium equal to 113.37 *veh*/0.5 *min*. However, the FHOCPs based on the PWA-CTM are showing faster convergence with much less error at the beginning of the simulation. The interesting result is that the network flow rate of the last two problems look to be the completely the same. To have a closer look at this comparison, the boxplot of the difference between the network flow rate of these two problems is provided in Fig. 7. It is clear that this difference is so small that can be neglected without any loss of generality.

Another factors used to evaluate the performance of these problems is the computation time and the number of iter-

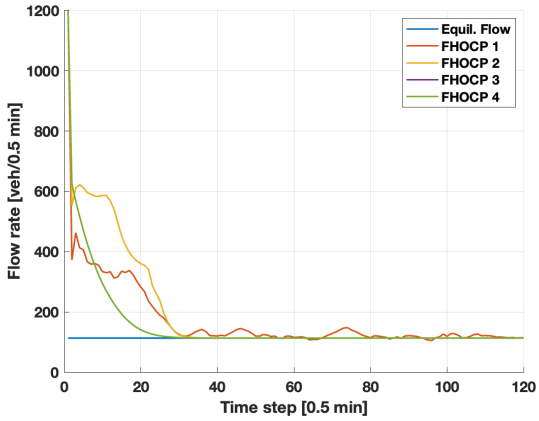

Fig. 6: Comparison of the network flow rate in all four problems.

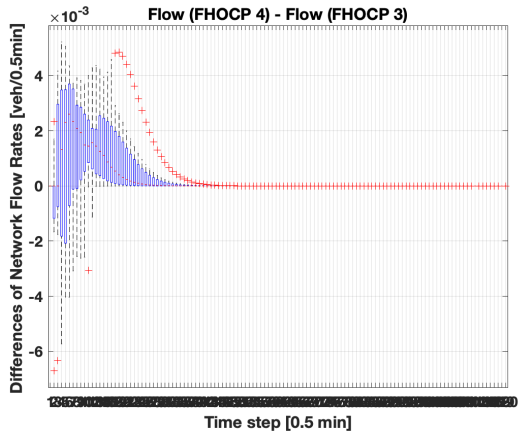

Fig. 7: Boxplot comparison of the network flow rate in problems based on the PWA-CTMs.

ations needed to solve each of the four problems. Table V shows the numerical value of these two factors. The value of these factor for the problem based on the Extended CTM is highly greater than those of the other problems. The reason is the large number of the nonlinear *min* function constraints in this model [9]. Also, considering the computation time of the other three problems, it can be seen that they almost have similar values, however, still the number of iterations needed to find a solution for the problems based on the PWA-CTM is much less and indicates that these optimization problems remain more tractable for real-time application of ramp metering optimal controllers.

TABLE V: Comparison of the Computation Times and Iteration Numbers.

Problem	Computation Time (sec)	Iterations
FHOCP 1	245.88	618713
FHOCP 2	1.53	4212
FHOCP 3	1.62	746
FHOCP 4	1.64	749

The evolution of the ramp metering variables are also investigated here. Fundamentally, the expectation is that the control applied to the on-ramps can satisfy the requirements of the network while considering the external demand of the on-ramps by not imposing too much waiting time to the vehicles on the on-ramps. As a result, a proper RM variable basically should replicate the overall demand pattern of that on-ramp. As an example, Fig. 8 shows the RM variable of on-ramp $o3$. In all four problems, the control variable is trying to converge to the value of the external demand applied (a constant demand of 7 *veh*/0.5 *min*). However, the RM variable in problems based on PWA-CTM have smoother and faster convergence with much less fluctuations while the control variable in the problem based on the Extended CTM never actually converges and in the problem based on the Relaxed CTM, a big overshoot happens before it starts to converge.

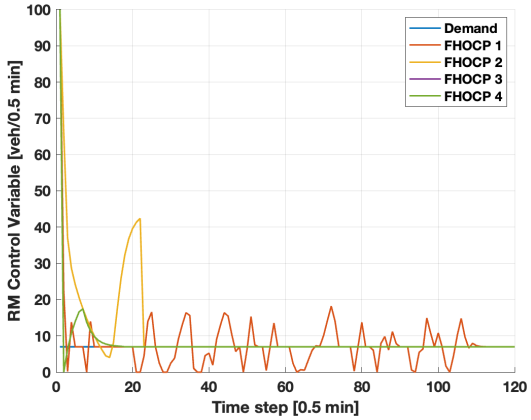

Fig. 8: Evolution of the RM control variable of on-ramp $o3$.

Last but not least, the MSE between the network flow rate and density of the problems is compared with that of the equilibrium state. The results are provided in Fig. 9. The problem based on the Relaxed CTM has the highest MSE for both the flow rate and density of the network. It is because of the crude simplifications made in this version of the CTM [9]. Comparing the MSE of the problem based on the Extended CTM and the performance of the problems based on the PWA-CTM, the results show less MSE for the last two FHOCPs. It indicate the FHOCPs based on the PWA-CTM have less error comparing to the equilibrium values of the flow rate and density.

VI. Conclusion

In this study, two enhanced CTM versions are proposed which constitute the PWA approximations of the flow-density relation of the FD. Most of the other extensions of CTM are based on the trapezoidal approximation of this relation in order to simplify optimization problems based on them. However, the flow-density relation is naturally nonlinear, and primitive approximations highly affect the efficiency of the optimization solution. The PWA approximation proposed here is computed based on a two-step identification method

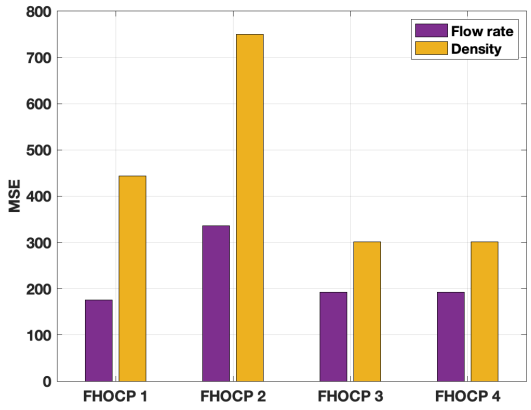

Fig. 9: Bar plot comparison of the MSE of the network flow rate and density.

to minimize the integrated squared error with respect to the true relation. The so-called PWA-CTM versions are evaluated in the framework of FHOCPs for a hypothetical highway network using the PI-ALINEA RM strategy. Also, for better evaluation, the performance of these models are compared with that of two other widely used versions of the CTM in the same optimization framework. Simulation results of these FHOCPs show that the problems based on the PWA-CTM models require less computation time and less iteration numbers compared to other problems. In addition, the problems based on the PWA-CTM models indicate higher accuracy of the flow and density evolution in comparison with the theoretical equilibrium state of the network. Also, the optimization problems based on the PWA-CTMs remains tractable for real-time application of ramp metering optimal controllers. Hence, the proposed PWA-CTMs constitute one of the best approximation approaches for first-order traffic flow models suitable for more challenging modeling and control applications. In future, authors intend to compare and evaluate the performance of the PWA-CTMs with the "Simulation of Urban MObility" (SUMO) traffic simulator for larger-scale highway networks.

REFERENCES

[1] R. C. Carlson, I. Papamichail, M. Papageorgiou, and A. Messmer, "Optimal motorway traffic flow control involving variable speed limits and ramp metering," *Transportation science*, vol. 44, no. 2, pp. 238–253, 2010.

[2] Z. Liu, Y. Wu, S. Cao, L. Zhu, and G. Shen, "A ramp metering method based on congestion status in the urban freeway," *IEEE Access*, vol. 8, pp. 76 823–76 831, 2020.

[3] Y. Bie, M. Seraj, C. Zhang, and T. Z. Qiu, "Improving traffic state prediction model for variable speed limit control by introducing stochastic supply and demand," *Journal of Advanced Transportation*, vol. 2018, 2018.

[4] F. van Wageningen-Kessels, H. Van Lint, K. Vuik, and S. Hoogendoorn, "Genealogy of traffic flow models," *EURO Journal on Transportation and Logistics*, vol. 4, no. 4, pp. 445–473, 2015.

[5] J. Hueper, G. Dervisoglu, A. Muralidharan, G. Gomes, R. Horowitz, and P. Varaiya, "Macroscopic modeling and simulation of freeway traffic flow," *IFAC Proceedings Volumes*, vol. 42, no. 15, pp. 112–116, 2009.

[6] M. J. Lighthill and G. B. Whitham, "On kinematic waves i. flood movement in long rivers," *Proceedings of the Royal Society of London. Series A. Mathematical and Physical Sciences*, vol. 229, no. 1178, pp. 281–316, 1955.

[7] C. Daganzo, "The cell transmission model part i: a simple dynamic representation of higheay traffic," *PATH Report, 93-0409*, vol. 3, 1993.

[8] A. Ferrara, S. Sacone, and S. Siri, *Freeway traffic modelling and control*. Springer, 2018.

[9] F. Alimardani and J. S. Baras, "Performance assessment of different cell-transmission models for ramp-metered highway networks," *IFAC-PapersOnLine*, vol. 54, no. 2, pp. 114–120, 2021.

[10] G. Gomes and R. Horowitz, "Optimal freeway ramp metering using the asymmetric cell transmission model," *Transportation Research Part C: Emerging Technologies*, vol. 14, no. 4, pp. 244–262, 2006.

[11] R. T. Underwood, "Speed, volume, and density relationships," 1960.

[12] L. Ambühl, A. Loder, M. Bliemer, M. Menendez, and K. W. Axhausen, "A functional form for the macroscopic fundamental diagram with a physical meaning," *Arbeitsberichte Verkehrs-und Raumplanung*, vol. 1306, 2017.

[13] C. F. Daganzo, "The cell transmission model: A dynamic representation of highway traffic consistent with the hydrodynamic theory," *Transportation research part B: methodological*, vol. 28, no. 4, pp. 269–287, 1994.

[14] B. D. Greenshields, J. Thompson, H. Dickinson, and R. Swinton, "The photographic method of studying traffic behavior," in *Highway Research Board Proceedings*, vol. 13, 1934.

[15] H. Greenberg, "An analysis of traffic flow," *Operations research*, vol. 7, no. 1, pp. 79–85, 1959.

[16] G. F. Newell, "Nonlinear effects in the dynamics of car following," *Operations research*, vol. 9, no. 2, pp. 209–229, 1961.

[17] M. C. Bliemer and M. P. Raadsen, "Continuous-time general link transmission model with simplified fanning, part i: Theory and link model formulation," *Transportation Research Part B: Methodological*, vol. 126, pp. 442–470, 2019.

[18] C. F. Daganzo and N. Geroliminis, "An analytical approximation for the macroscopic fundamental diagram of urban traffic," *Transportation Research Part B: Methodological*, vol. 42, no. 9, pp. 771–781, 2008.

[19] M. Carey and M. Bowers, "A review of properties of flow–density functions," *Transport Reviews*, vol. 32, no. 1, pp. 49–73, 2012.

[20] Y. Wang, E. B. Kosmatopoulos, M. Papageorgiou, and I. Papamichail, "Local ramp metering in the presence of a distant downstream bottleneck: Theoretical analysis and simulation study," *IEEE Transactions on Intelligent Transportation Systems*, vol. 15, no. 5, pp. 2024–2039, 2014.

[21] J. Stevek, A. Szucs, M. Kvasnica, M. Fikar, and S. Kozák, "Two steps piecewise affine identification of nonlinear systems," *Archives of Control Sciences*, vol. 22, no. 4, pp. 371–388, 2012.

[22] G. Gomes, R. Horowitz, A. A. Kurzhanskiy, P. Varaiya, and J. Kwon, "Behavior of the cell transmission model and effectiveness of ramp metering," *Transportation Research Part C: Emerging Technologies*, vol. 16, no. 4, pp. 485–513, 2008.

[23] J. Löfberg, "Yalmip: A toolbox for modeling and optimization in matlab," in *In Proceedings of the CACSD Conference*, Taipei, Taiwan, 2004.